7-14-2013

Monitoring Aircraft Cabin Particulate Matter Using a Wireless Sensor Network

James A. Hall Jr.
Boise State University

Joshua Kiepert
Boise State University

Michael Pook
Boise State University

Sin Ming Loo
Boise State University

Monitoring of Aircraft Cabin Particulate Matter Concentrations Using a Wireless Sensor Network

James A. Hall Jr.[1], Joshua Kiepert[2], Michael Pook[3], Sin Ming Loo[4]
Boise State University, Boise, Idaho, 83725

The semi-enclosed and pressurized nature of the aircraft cabin results in a highly dynamic environment. The dynamic conditions establish spatiotemporal dependent environmental characteristics. Characterization of aircraft cabin environmental and bleed-air conditions have traditionally been done with stand-alone measurement systems which, by their very nature, cannot provide the necessary sensor coverage in such an environment. To this purpose, a prototype wireless sensor network system has been developed that can be deployed in the aircraft cabin environment. Each sensor node in the system incorporates the ability to measure common aircraft contaminants such as particulate matter and carbon dioxide, along with other key environmental factors such as temperature, air pressure, humidity, and sound pressure level. The wireless sensor network enables the collection of time-correlated results from the aircraft cabin, passing sensor data to a central collection point for storage or real-time monitoring. This paper discusses the results of testing this sensor system in a mockup of the Boeing 767 aircraft cabin environment. In this series of tests, both particulate matter and carbon dioxide were introduced into the simulated aircraft environment and measured using an array of 16 wirelessly connected sensor nodes. Two different arrangements of sensor nodes targeted both a two-dimensional plane across the aircraft cabin space and a localized three-dimensional space centered on two rows of the cabin. The test results show successful simultaneous tracking of the particulate matter and carbon dioxide concentrations as they disperse over time.

I. Introduction

THE quality of the air that we breathe is one of the more noticeable conditions of our environment that impacts comfort and health. Maintaining good air quality quickly becomes very important when one cannot simply step outside or open a window for fresh air. The confined spaces and close proximity to neighboring passengers encountered in aircraft cabins present many challenges for maintaining appropriate air quality[1]. This coupled with the potential for contaminants brought into the aircraft from outside can impact comfort and health in many ways[2,3]. Concern with the microbial content of cabin air has led to multiple studies regarding infectious disease transmission on aircraft[4–6]. Increased understanding of these complex spaces can be realized through the use of advanced approaches to air quality monitoring, fusing measurements of particulate matter and contaminant gasses to create an enhanced view of this dynamic environment.

On September 13th 2012, Boise State University (BSU) deployed its Wireless Air Quality Monitor (WAQM) wireless sensor network within the Kansas State University (KSU) Boeing 767 mock-up cabin. The focus of this testing was to verify the capabilities of the BSU system in capturing spatiotemporal measurements of multiple contaminants injected into a highly dynamic enclosed environment. Previous testing of a similar system had focused on capturing the movement of carbon dioxide in the same environment[7]. This set of tests demonstrates the addition of particulate matter sensing to the sensor suite, providing contrast between the movement of gaseous and particulate matter contaminants.

The deployment of the WAQM sensor network consisted of 16 wireless sensor units and a coordinating base station. Each wireless sensor unit was configured to measure five environmental conditions: airborne particulate matter, CO_2, temperature, humidity, and atmospheric pressure. For testing in the aircraft cabin, two different node

[1] Graduate Student, Electrical and Computer Engineering, 1910 University Dr. MS2075
[2] Graduate Student, Electrical and Computer Engineering, 1910 University Dr. MS2075
[3] Graduate Student, Electrical and Computer Engineering, 1910 University Dr. MS2075
[4] Professor and Department Chair, Electrical and Computer Engineering, 1910 University Dr. MS2075

arrangements were exercised. First, the sixteen sensor nodes were set out in a two-dimensional array on the tops of the seat backs in the cabin. The goal of this test was to cover most of the cabin area with sensors to show large scale movement of gas and particulate matter within the space. The second arrangement concentrated the nodes at two vertical levels across a pair of rows near the front of the cabin. This more dense arrangement was used to show finer scale movement within a smaller area in three dimensions.

In the sections of this paper that follow, descriptions of the simulated aircraft cabin environment (Section II) and the WAQM sensor network (Section III) will be given. Results are then presented from the two-dimensional (Section IV) and three-dimensional (Section V) testing. This paper is based, in part, upon the FAA Airliner Cabin Environment Research report RITE-ACER-CoE-2013-TBD[8] and the results presented therein.

II. Simulated Aircraft Cabin Environment

A typical commercial aircraft cabin is an enclosed, ventilated space with a dedicated environmental control system. Occupants of the aircraft are exposed to a mixture of recirculated and outside air, usually supplied by a bleed air compressor system on the engines. The air quality in the aircraft cabin is dependent on the environmental control system to filter contaminants entering from outdoor air and to dilute and filter contaminants generated in the cabin. These contaminants can range from urban pollution such as particulate matter and carbon monoxide encountered at the airport or during ascent/descent, to ozone encountered at cruising altitude, to particulate matter and carbon dioxide generated inside the cabin[1]. The dynamic nature of the combined system of forced ventilation, changing air pressure, and diverse contaminant sources in an actively-used aircraft provides a challenging situation for effective environmental monitoring. The availability of a controlled, simulated aircraft cabin environment is important to the development of such systems.

The KSU aircraft cabin section is designed to simulate the interior conditions of a portion of a Boeing 767. The cabin contains two aisles and eleven rows of seven seats arranged in a 2-3-2 configuration. The interior space is approximately 9.6 meters long by 4.7 meters wide by 2.0 meters high and is modeled in shape similar to the actual aircraft. Each seat in the cabin is occupied by a simulated human in the form of a mannequin. These mannequins include heating elements to mimic the body heat produced by an actual passenger. Figure 1 shows a view from the rear of the interior of the aircraft cabin with the WAQM sensor nodes in place on the seatbacks.

Ventilation for the aircraft cabin is provided by an air supply system that takes in air from outside the test facility. This air is first taken through HEPA filters to remove ambient particulate matter and a dehumidifier controls the amount of moisture in the air. The air is also conditioned for temperature with heating and cooling elements. Air enters the cabin from a set of diffusers in the ceiling arranged above the center section of seats. Gaps along the floor on both sides of the cabin allow air to exit as it would on an actual aircraft. The air is not recirculated once it exits the cabin, and is instead replaced by fresh air from the ventilation system.

At the time of testing, two different types of contaminants were available to be released into the cabin: CO_2 and particulate matter. The CO_2 source was a cylinder of compressed gas with a regulated output. When active, the CO_2

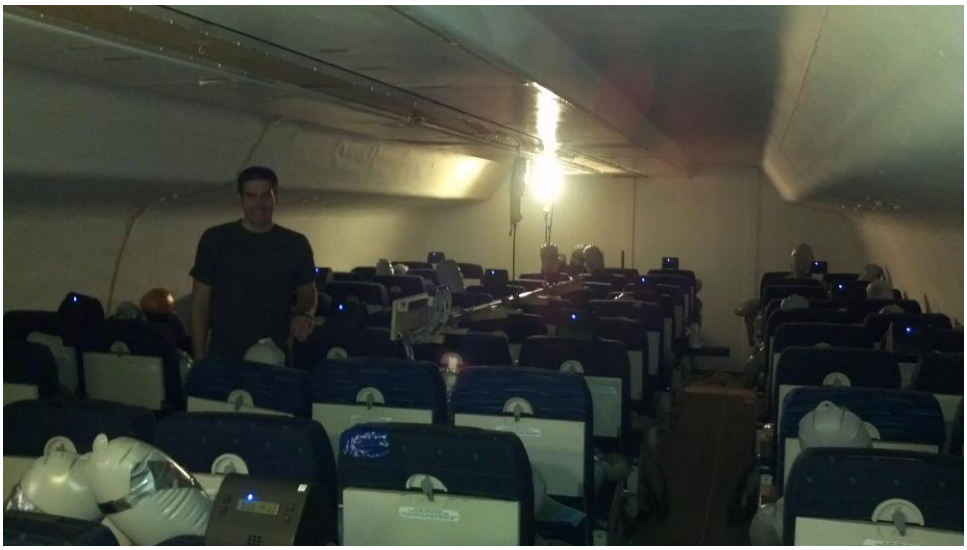

Figure 1: Interior of the aircraft cabin mockup with WAQM sensors in place for two-dimensional testing.

source releases 7 liters/minute of undiluted gas. The CO_2 is piped into the aircraft cabin to a single point at the front of the cabin where it is then released into the air.

The KSU system has two different methods for generating particulate matter. The first method generates smoke through a Chauvet Hurricane 1050 commercial fog generator using an aerosolized mixture of propylene glycol and glycerin. This system typically produces a large number of small particles with diameters less than 2.5um. The particulate from the fog generator is introduced into the cabin using the same pipe that carries the CO_2. During each run that it is used the fog generator remains active for approximately five minutes and is then shut down, allowing the particulate to clear from the cabin. The second particulate generation method uses talcum powder and a series of seven air nozzles that disperse the powder from small containers placed at each seat across a single row. The talcum powder particulate is released in a single burst of air. Compared to the fog generator this method produces a much smaller total amount of particulate matter with a larger distribution in sizes, with some particles reaching diameters greater than 10 um.

III. Sensor Network

The Boise State University WAQM system was initially developed as part of a project for the National Institutes of Health National Children's Study[9]. Continued development with funding from the Federal Aviation Administration is targeting the system for bleed-air monitoring in aircraft cabins.

Each sensor node in the WAQM system is equipped to measure particulate matter, CO_2, CO, humidity, pressure, temperature, and sound pressure level. The sensor nodes can run from an internal lithium-ion battery or from a wall transformer. Data collected by each node can be stored locally on the device and/or sent through the integrated ZigBee mesh network to a central coordinator node. Figure 2 shows one of the WAQM sensor nodes used in the testing.

Figure 2. In-Home Air Quality Monitor. *The monitor measures 150x150x115 mm and weighs 700g.*

Sixteen WAQM sensor nodes and one coordinator node were used for testing in the KSU simulated aircraft cabin. Each of the sensor nodes was configured identically, with sensors set to report data according to Table 1. Note that some of the sensors in each node were not used, either because the particular contaminant was not of interest in this testing environment or to conserve mesh network bandwidth and system power. Particulate matter count was set to a relatively high sample rate to provide good temporal resolution. The CO_2 sensor was set to a longer period since the particular brand of sensor used could not meet a 2-second sample rate.

Table 1: Controlled environment testing sensor configuration.

Sensor	Sample Period
CO	Disabled
CO2	5 seconds
Humidity	5 seconds
Particulate concentration	60 seconds
Particulate count	2 seconds
Performance	Disabled
Pressure	5 seconds
ZigBee radio status	30 seconds
Sound	Disabled
Temperature	5 seconds
Battery voltage	30 seconds

Bandwidth was of particular concern due to the number of nodes involved and the amount of data being sampled. The ZigBee mesh network offers a relatively low-bandwidth connection, and overtaxing it could lead to data loss at the coordinator. A backup system of local node logging was in place in case this occurred, but in the end no significant data loss was experienced by the mesh network.

Each of the sensor nodes was powered from its internal lithium polymer battery during the tests. This greatly simplified the setup of the system but caused some issues with data loss towards the end of testing. One unit in particular had a battery that performed much worse than the other units due to its age, causing the unit to power down just prior to the end of testing.

The coordinator node was connected to a monitoring computer using a serial cable that was passed under the door of the simulated aircraft cabin. The monitoring computer was used to verify correct operation of the sensor

network and to allow the operators to understand when contaminants had been flushed from the cabin at the end of each test. The monitoring computer also stored the aggregated data from the coordinator for later processing.

IV. Two-Dimensional Test Results

The first set of tests arranged nodes in a two-dimensional 4x4 array across the body of the simulated cabin as shown in Figure 3. The goal of this arrangement was to cover as much of the cabin as possible at a level near the typical head-height of the passengers. Each node is shown as a green circle with the unit's position reference number indicated inside the circle. A set of four nodes was placed on the top of the seat-backs every three rows. Spacing between the units was approximately 130 cm between each column of units and 250 cm between each row of units. Particulate matter and CO_2 were injected into the cabin from a single contaminant injection point approximately 10 cm above the top of the seat backs as indicated by the red triangle in Figure 3. The coordinator node for the mesh network was located near the back of the cabin as indicated by the blue pentagon.

The CO_2 and particulate matter were released into the cabin concurrently six times over the course of three and one-half hours. Table 2 lists the tests conducted for the two-dimensional setup, with references for each of the six tests listed in the leftmost column of the table.

The first test, run 0, was performed as a check of the system operation. The sensor unit hardware had been shipped to the testing facility and needed to be tested for correct operation after unpacking. During this run it was discovered that the unit at position 12 had a malfunctioning particle counter and was

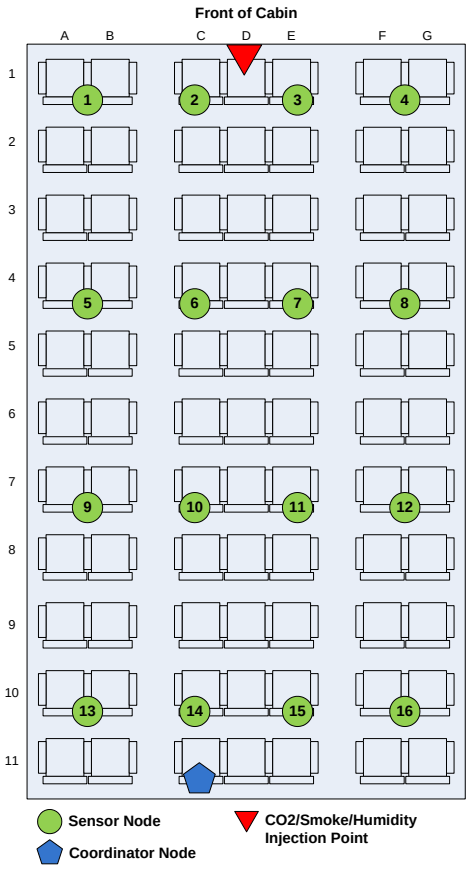

Figure 3: WAQM sensor node layout for two-dimensional test.

Table 2: Two-dimensional testing sequence of events.

Reference	Variables	Log (UTC Time)	Comments
Run 0	Particulate (smoke) CO_2 Dehumidifier active Humidifier inactive	14:30: Start CO_2, smoke release 14:47: Stop CO_2	Initial test to verify sensor network formation and general operation. Position 12 (Unit 74) found to have malfunctioning particle counter.
Run 1	Particulate (smoke) CO_2 Dehumidifier active Humidifier inactive	15:08: Start CO_2, smoke release 15:28: Stop CO_2	First full run. Unit 74 replaced with Unit 79.
Run 2	Particulate (smoke) CO_2 Dehumidifier active Humidifier inactive	15:43: Start CO_2, smoke release 16:09: Stop CO_2 16:11: Stop dehumidifier	Second full run.
Run 3	Particulate (smoke) CO_2 Dehumidifier inactive Humidifier active	16:25: Start CO_2, smoke release, humidifier on 16:50: Stop CO_2	Dehumidifier turned off. Humidifier appears to modify air currents around CO_2/particulate cabin input.
Run 4	Particulate (smoke) CO_2 Dehumidifier inactive Humidifier active	17:03: Start CO_2, smoke release 17:18: Stop CO_2	Repeat of Run 3 conditions. Humidifier remained active since the start of Run 3.
Run 5	Particulate (smoke) CO_2 Dehumidifier inactive Humidifier inactive	17:26: Stop Humidifier 17:29: Start CO_2, smoke release 17:29: Battery died on Unit 60 17:45: Stop CO_2	Same conditions as Run 4, with humidifier inactive. Confirm humidifier modifies CO_2, likely due to air current changes.

replaced with a backup unit before continuing with run 1.

Figure 4 shows the time-series data for the particulate matter concentration plotted on a logarithmic scale. All sixteen units are shown concurrently to give an idea of the distribution seen across the different sensing positions. The concentrations tend to be higher towards the front of the aircraft cabin where the particulate matter is injected into the environment and fall off moving towards the rear. The largest peaks in particulate matter concentration approach 10 million particles per liter when smoke is being actively injected into the cabin and fall off to 1000 particles per liter or lower in-between testing.

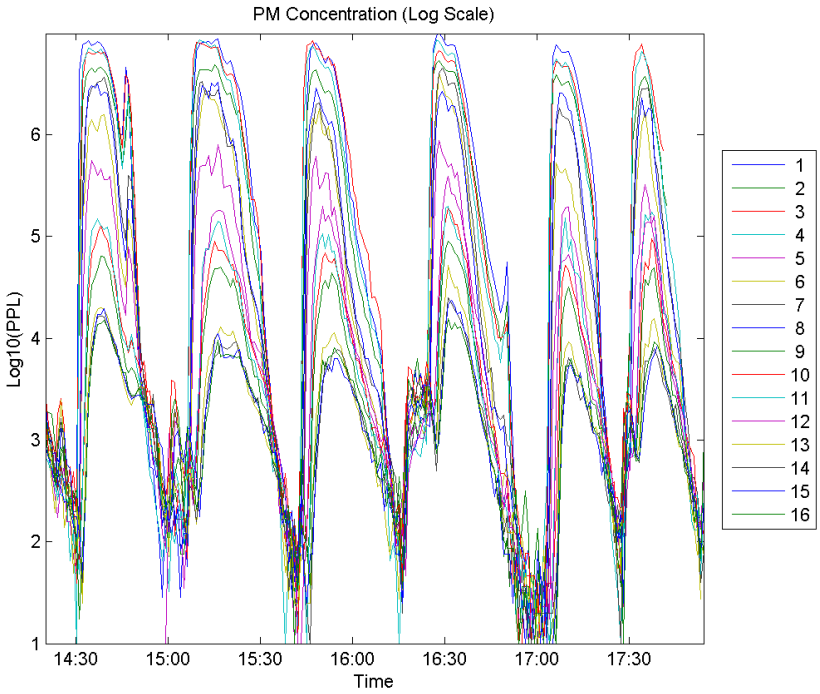

Figure 4: Two-dimensional test particulate matter concentration in particles per liter for all sixteen sensor nodes on a logarithmic scale.

Note that the particulate matter level between test runs tends to reflect activity in the cabin. For example, the humidifier was set up in the cabin at approximately 16:20 prior to run 3. The doors to the cabin were opened and several people entered, raising the particulate matter concentration as existing particulate was stirred up and new particulate entered through the doors. In contrast, no one entered the cabin in between run 3 and run 4 at approximately 17:00 hours. In this case the particulate falls to a very low level as the particulate-laden air from testing is replaced by clean air from the ventilation ducts.

The time-series data for the CO_2 concentration is shown in Figure 5. As with the particulate matter, concentrations tend to be most intense at the front of the cabin near the contaminant injection point and fall off toward the rear. Of particular interest here is the behavior of the sensor node at position 3. This node was located at the front of the cabin very near to the contaminant injection point and apparently received high concentration doses of the gas as it flowed into the space. With the introduction of the humidifier at the front of the cabin prior to run 3, the CO_2 concentration seen by this node fell off drastically. This appeared to be due to the forced air from the humidifier shifting the air currents in the cabin, deflecting the high levels of CO_2 from this sensor node when running. This theory was tested by turning off the humidifier for run 5, which caused the high concentrations at position 3 to return.

As noted in the discussion on the particulate matter time-series plot, the humidifier was installed in the cabin at approximately 16:20. Two individuals were working on this activity for several minutes in the aisle between positions 2 and 3. In Figure 5, the CO_2 exhalations of the two individuals involved in this activity can be observed as the small peak in concentration at position 2.

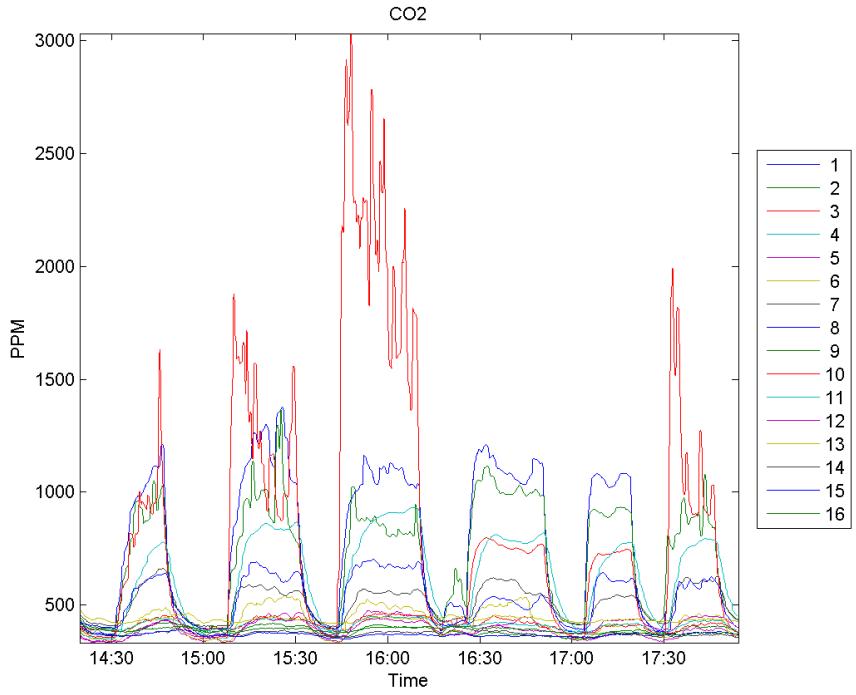

Figure 6: Two-dimensional test CO_2 concentration in parts per million for all sixteen sensor nodes on a linear scale.

Looking at the contour data across the cabin provides further insight into the distribution and movement of the particulate matter and CO_2. Figure 6 shows two contour plots along with a time-series plot. The contour plot on the left shows the particulate matter count across the area of the aircraft cabin, with row numbers along the left and seat letters along the bottom. Similarly, the contour plot on the right shows the CO_2 concentration in the cabin. Both contour plots use a logarithmic scale to better highlight the concentrations across the entire range that was seen during testing. The two contour plots show the data from the time indicated with the vertical black line in the time-series plot on the far right. This time-series plot of particle counts corresponds to the particulate matter concentration plot of Figure 4. The contour plots both show relatively low concentrations of both particulate matter and CO_2 in the cabin just before the contaminants are released into the cabin.

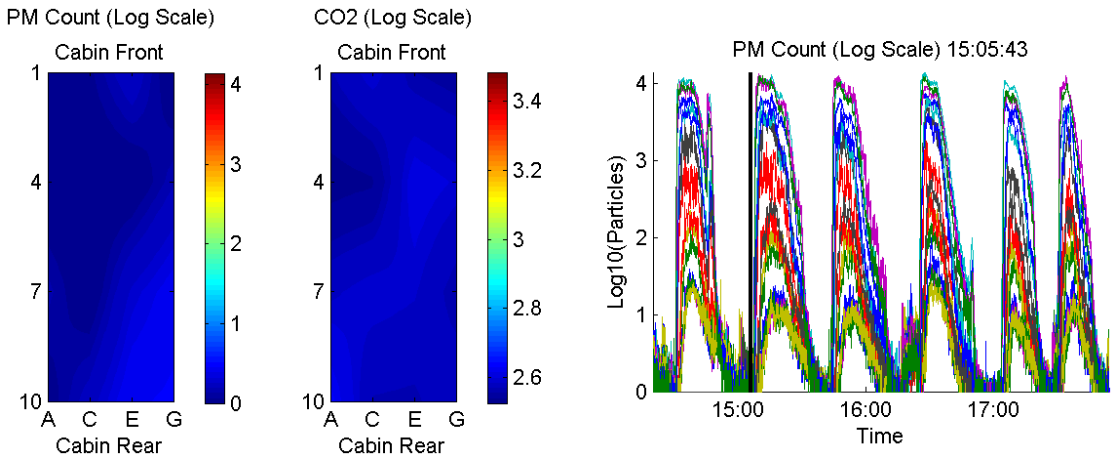

Figure 5: Two-dimensional tests with particulate and CO_2 contour plots just prior to Run 1.

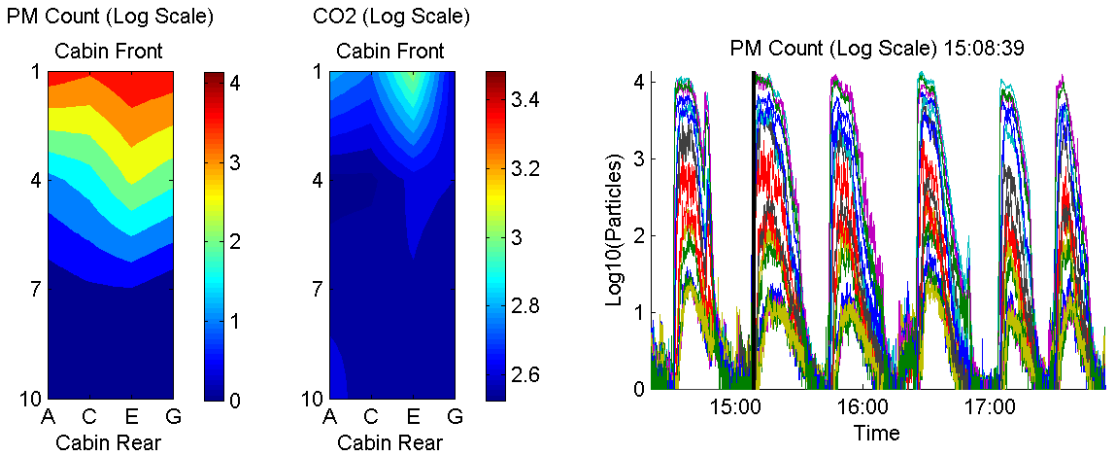

Figure 7: Two-dimensional tests with particulate and CO2 contour plots at the beginning of contaminant dispersal.

The time just after the contaminants are introduced into the cabin is shown in Figure 7. It is immediately apparent that there is a large difference between the spread of the particulate matter and the CO_2 concentrations. While this may appear to be significant, it may be due to a difference in response times of the two sensors. The particulate matter sensor has a forced air system and will register an increase in particulate matter in as little as two seconds from the time it is pulled into the sensor's air intake. The CO_2 sensor on the other hand has a response time that is specified as being less than two minutes.

Figure 8 shows the concentrations at the peak of the contaminant dispersal during run 1. The particulate concentration is relatively high and spreads down the length of the cabin. It is apparent that the cabin airflow moves the contaminants across the width of the cabin much more effectively than down the length. Even more than six minutes from the first appearance of the particulate matter in the cabin, it has still not equalized down the length. The evacuation of air from the vents at the sides of the cabin must be removing the particulate before it can spread. Similarly, the CO_2 concentration spreads across the width of the cabin much more strongly than down the length.

Comparing the concentrations of the two contaminants, one can see a similar shape to the flow down the length of the cabin. It appears that there is more movement of contaminants along the right side (seats F and G) compared to the left (seats A and B) towards the rear of the cabin. The correlation between the two different sensors may indicate an actual difference in airflow. After a period of time the smoke from the fog generator starts to dissipate and the CO_2 is turned off at the source. Eventually, the contaminant is cleared from the cabin and conditions return to those similar to what is shown in Figure 6.

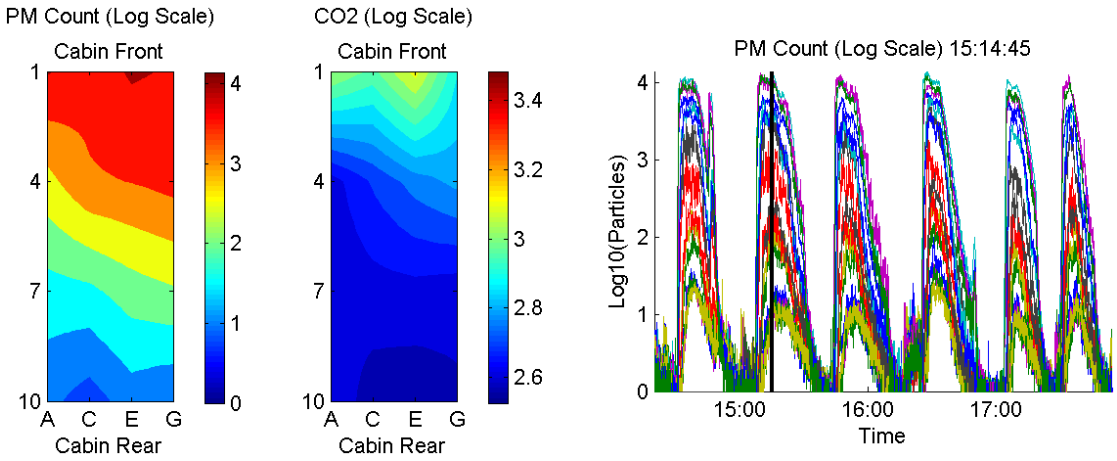

Figure 8: Two-dimensional tests with particulate and CO2 contour at the peak of contaminant dispersal.

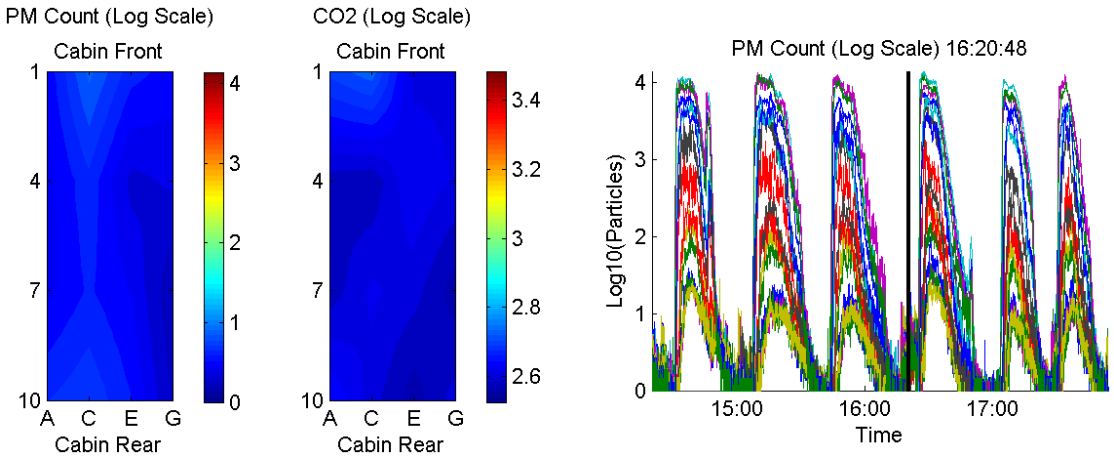

Figure 10: Two-dimensional tests with particulate and CO2 contours showing human activity in the aircraft cabin.

From the time-series plots of Figure 4 and Figure 5, we can see evidence of human activity in the cabin between runs. This can also be seen in the contour plots from the same time frame. The contour plot on the left of Figure 9 shows the introduction of particulate matter along the aisle on the left side of the aircraft cabin as the individuals move up and down this aisle while bringing the humidifier into the cabin. Note that the concentration is much lower than an event caused by the fog generator. The individuals were active at the front-left of the aircraft cabin as they worked to activate the humidifier. The contour plot on the right of Figure 9 shows this as an increase in CO_2 at this location as the individuals exhale. As with the particulate concentration, the CO_2 increase caused by the individuals is much lower than that of the pure CO_2 injection.

The impact of humidity on the contaminant movement in the cabin was also tested by turning off the dehumidifier in the ventilation system and adding a humidifier at the front of the cabin. The biggest impact of this change appears to be more due to the forced airflow of the humidifier than any impact of the moisture content of the air. This shows up mostly in the CO_2 concentration as it appears to remove the large peaks seen by the sensor node at position 3. This is presumably due to the change in airflow pushing the CO_2 away from the sensor at position 3. Figure 10shows the contour data from run 4. The intense peak of CO_2 is now missing from position 3, but there does not appear to be much else that is different from runs with low humidity. There is still the same increase in concentration on the right side of the cabin in comparison to the left with both contaminants. Run 5, the final run of the test period, was executed with the humidifier turned off to verify that the CO_2 peaks would return to the sensor node at position 3. This was the case, which can be most clearly seen in Figure 5.

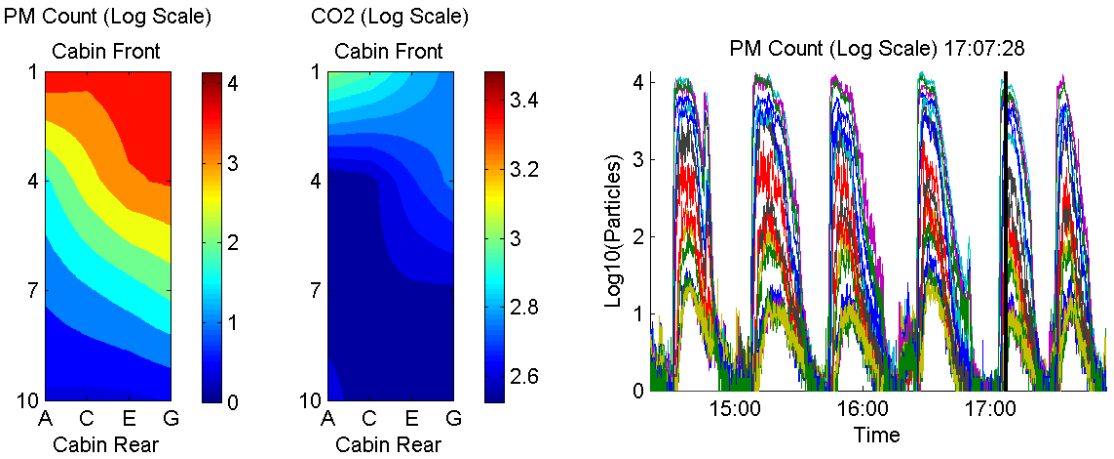

Figure 9: Two-dimensional testing with the dehumidifier off and the humidifier on.

V. Three-Dimensional Test Results

The second set of tests arranged sixteen nodes in a 4x2x2 three-dimensional array at the front of the cabin with two vertical layers covering two rows of seats. The goal of this arrangement was to cover an area near the contaminant injection point with a dense matrix of nodes in an attempt to look at the three-dimensional movement of particulate and CO_2 in the aircraft cabin. Figure 11 shows the layout of the sensor nodes in the cabin for this test, with the head-height layer at top and the tray-height layer at the bottom. The top layer of sensor nodes was suspended from the ceiling at a height above head level for a seated passenger, and the bottom layer was placed on the tray table of each seat. Spacing between the units was approximately 130 cm between each of the four columns of units, 80 cm between the two rows of units, and 80 cm between the two vertical layers. As with the two-dimensional test, CO_2 and particulate matter from a fog machine were injected at the front of the cabin. Additionally, the talcum powder dispersion system was tested that had injection points across the second row of seats in the cabin. The mesh network coordinator node remained at the rear of the cabin, passing data to an external computer over a serial cable.

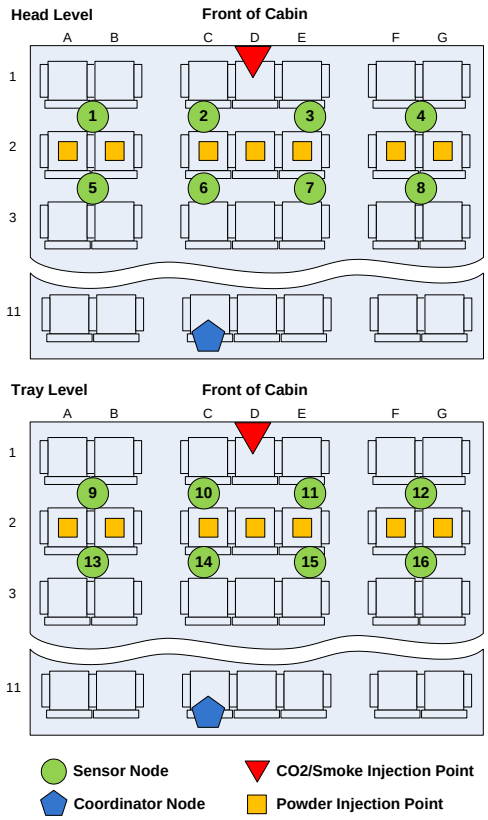

Figure 11: WAQM Sensor Node Layout for Three-Dimensional Test.

The CO_2 and particulate matter from the fog machine were released into the cabin concurrently three times during the first part of the testing period. During the latter portion of the testing period, the talcum powder dispersion system was used to release particulate matter into the cabin twice without the injection of CO_2. Table 3 lists the tests conducted for the three-dimensional setup, with references for each of the five tests listed in the leftmost column of the table. The dehumidifier was on for all tests except for run 4, and the humidifier remained off for the entire set.

Figure 12 shows the time-series plot of the particulate matter concentration for the three-dimensional testing plotted on a logarithmic scale. The first three large peaks correspond to runs 1, 2, and 3 in Table 3, in which a fog

Table 3: Three-dimensional testing sequence of events.

Reference	Variables	Log (UTC Time)	Comments
Run 1	Particulate (smoke) CO_2 Dehumidifier active Humidifier inactive	20:00: Start CO_2, smoke release 20:15: Stop CO_2	First test of 3-D arrangement.
Run 2	Particulate (smoke) CO_2 Dehumidifier active Humidifier inactive	20:28: Start CO_2, smoke release 20:45: Stop CO_2	Second test of 3-D arrangement. Units at positions 11 and 16 swapped.
Run 3	Particulate (smoke) CO_2 Dehumidifier active Humidifier inactive	20:55: Start CO_2, smoke release 21:14: Stop CO_2	Third test of 3-D arrangement.
Run 4	Particulate (talcum) Dehumidifier inactive Humidifier inactive	21:25: Door open (powder load) 21:31: Door closed 21:33: Powder released	First talcum powder based particulate test.
Run 5	Particulate (talcum) Dehumidifier active Humidifier inactive	21:45: Door open (powder load) 21:49: Door closed 21:09: Powder released	Second talcum powder based particulate test.

generator was used for the injection of particulate matter. These tests exhibit curves similar to what was seen in the two-dimensional testing. The last three large peaks correspond to testing with talcum powder. Note that the first of these talcum powder peaks was a demonstration using just a single of the seven talcum powder dispersal locations, and is not considered a formal test. The remaining two peaks correspond to runs 4 and 5 in Table 3. Note that the fog generator creates peaks in particulate matter that are nearly two orders of magnitude higher in concentration than the talcum powder dispersal system. The talcum powder peaks are also much shorter in duration, since they are released in a burst and have no sustained source of generating material.

Compared with the two-dimensional testing, the particulate matter concentrations for the three-dimensional tests are much closer in magnitude across the set of sensor nodes. This is likely due to the close proximity of the nodes in the cabin for the three dimensional testing, especially in the direction of the axis of the airplane. Much of the variation between sensor nodes in the two-dimensional tests came from the change in concentration down the length of the cabin. Since the layout of the nodes in the three-dimensional test only covers two rows in this direction, one

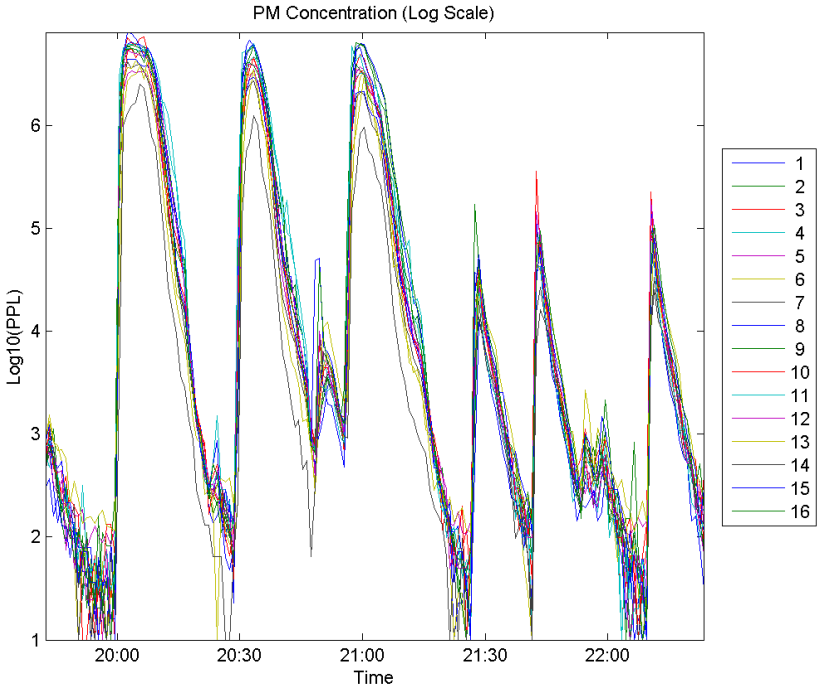

Figure 12: Three-dimensional test particulate matter concentration in particles per liter for all sixteen sensor nodes on a logarithmic scale.

might expect that the nodes would observe a smaller difference in concentration.

The time-series data for the CO_2 concentration is shown in Figure 13. As with the particulate data, there is less of a distribution of concentrations across the sensor nodes, likely due to the dense clustering near to the contaminant injection point. The node at position 11 exhibits very high spikes of CO_2 during the first three test runs. This is similar to what was seen with the node at position 3 during the two-dimensional testing and corresponds to roughly the same position though at the tray table level rather than at the top of the seat back. To make sure that this was not a phenomenon specific to the sensor node at this point, the sensors at positions 11 and 15 were swapped after run 1. The high concentration peaks followed the position and not the specific sensor node, verifying that this was likely due to proximity to the contaminant injection point.

The two smaller peaks in CO_2 concentration at approximately 21:30 and 22:00 were due to human activity in the aircraft cabin, as no CO_2 was released during the talcum powder testing. The highest concentrations came from positions 2 and 10 at the tray table and head height units at the front of the left aisle in the cabin. This corresponds to locations where individuals were working in the cabin in between test runs.

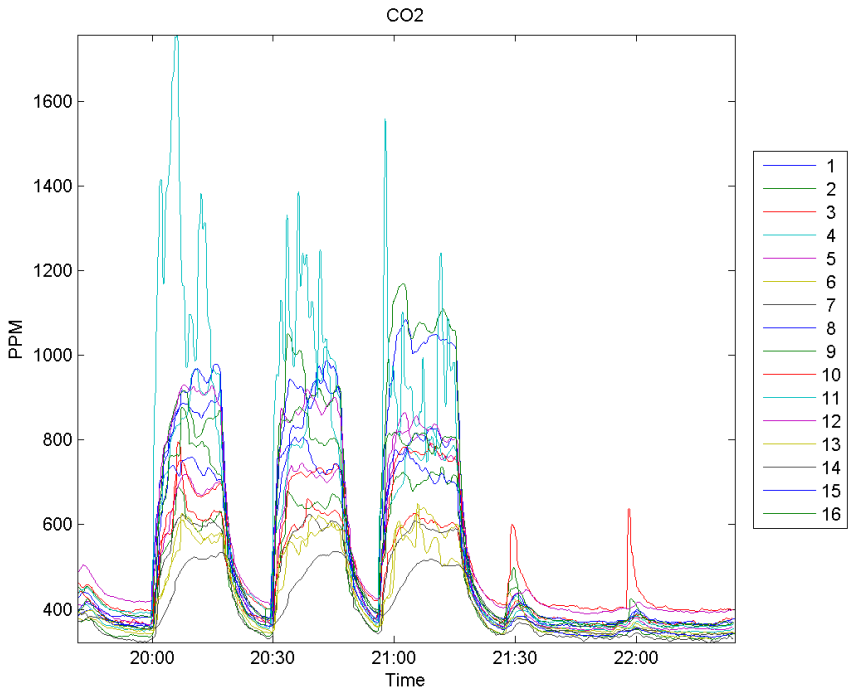

Figure 14: Three-dimensional test CO_2 concentration in parts per million for all sixteen sensor nodes on a linear scale.

The contour data for the three-dimensional testing is somewhat challenging to present. Figure 14 shows a set of four contour plots and two time-series plots. The plots on the left side of the figure show the particulate matter concentration, and those on the right show the CO_2 concentration. The two contour plots at the top of the figure show the particulate matter and CO_2 concentrations for head-level sensors, and the two contour plots in the middle show concentrations for the tray-level sensors. The black vertical line on each of the time-series plots shows the

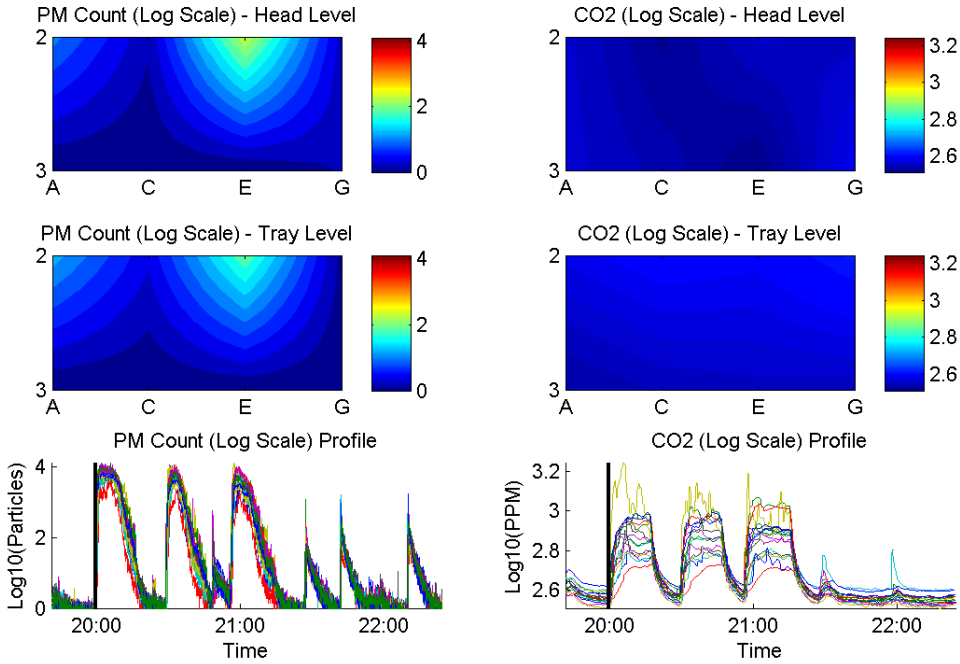

Figure 13: Three-dimensional smoke and CO_2 test with particulate and CO_2 contour plots at the beginning of contaminant injection.

point in time from which the contour plot data is taken. As with the two-dimensional contour data, the plots use a logarithmic scale to better highlight the concentrations across the entire range that was seen during testing. Figure 14 shows the concentrations of particulate and CO_2 at the start of contaminant injection for run 1. As with the two-dimensional testing, the particulate matter contaminant begins to appear earlier than the CO_2. This is likely due to sensor differences as explained above. The particulate matter first appears at sensor position nearest to the injection point at the front-center of the cabin. It is not clear why there is some initial response in particulate matter from the two sensors at the front-left of the cabin, but this appears to happen in runs 2 and 3 as well. It is possible that the airflow in the cabin is forcing some particulate into this corner early in the cycle, bypassing the sensors immediately to the left of the outlet.

The increase in particulate matter contaminant shows some interesting spatial trends early in the run. Figure 15 shows the particulate building up to higher concentrations toward the front of the cabin at both head and tray levels. The concentration has spread more quickly to the sides than across the seats into the third row. Also, the contaminant appears to have moved further to the right side of the cabin at the head-level, yet stays more concentrated around the injection point at the tray-level. This might be due to the ventilation inlet diffusers at the centerline of the ceiling pushing the particulate outwards nearer to the ceiling. The sensors are still not detecting the increase in CO_2 at this point in time.

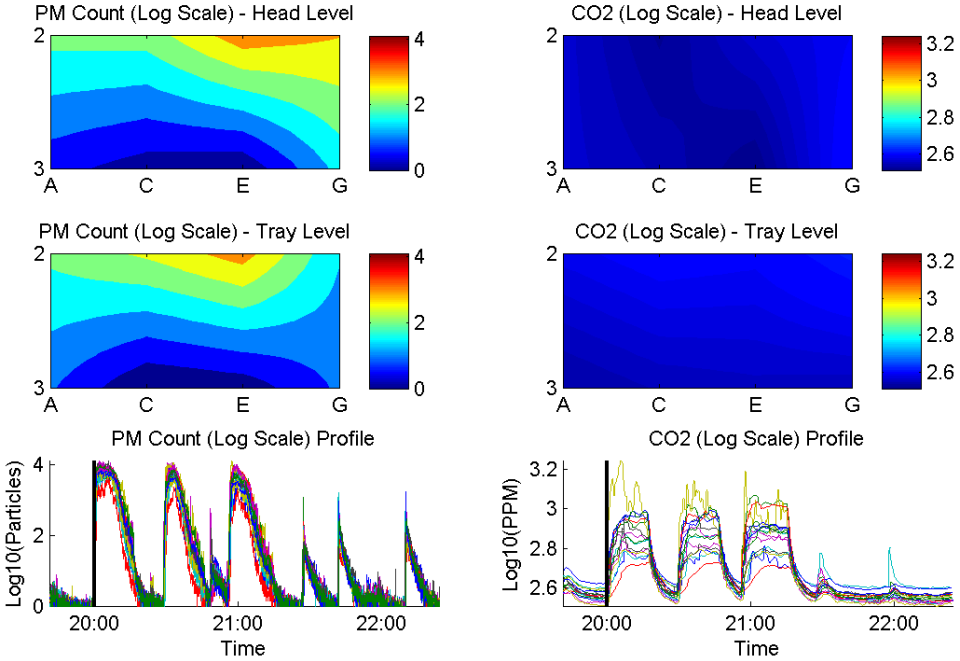

Figure 15: Three-dimensional smoke and CO_2 test with particulate and CO_2 contour plots as contaminant injection continues.

Figure 16 shows that, as the test run progresses, the sensors begin to register the increase in CO_2 concentrations in the cabin. The particulate matter has built up to relatively high concentrations in the cabin, tending to move more strongly to the right side of the cabin than the left and spreading laterally more quickly than down the length of the cabin. This increased concentration down the right side of the cabin matches what was seen across a larger area in the two dimensional testing. Also notable is the larger difference between highest and lowest concentrations at the tray-level in comparison to head-level. This may again be due to the seats inhibiting the airflow at the tray-level. The CO_2 concentration does not build at the head-level nodes in the same way that is seen with particulate matter when it first appears. The sensor at position 3 that saw an early peak in particulate matter does not register much of an increase in CO_2. This could be due to the lack of forced airflow in the CO_2 sensor or even the differences in height between the two sensor types within the sensor node.

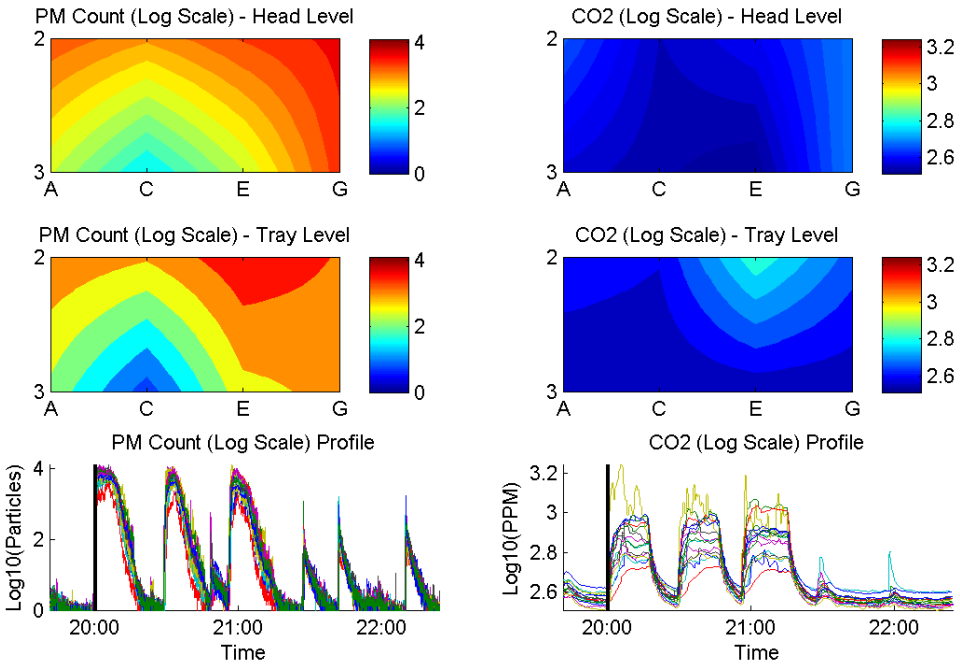

Figure 17: Three-dimensional smoke and CO_2 test with particulate and CO_2 contour plots as CO_2 begins to appear.

Figure 17 shows a view of the cabin at the peak of contaminant injection for run 1. The particulate matter has spread through the cabin, with marked differences between the left and right sides of the cabin. The concentration differences again appear larger at the tray-level than at head-level. The minimum in particulate matter at position 14 in row 3 on the left side of the cabin appears to be similar to the minimum seen in the CO2 data. While the large peaks in CO2 at position 11 tend to push the other contours down in scale, there does still appear to be a concentration that is more intense along the right side of the cabin. The CO_2 at head-level does appear to concentrate

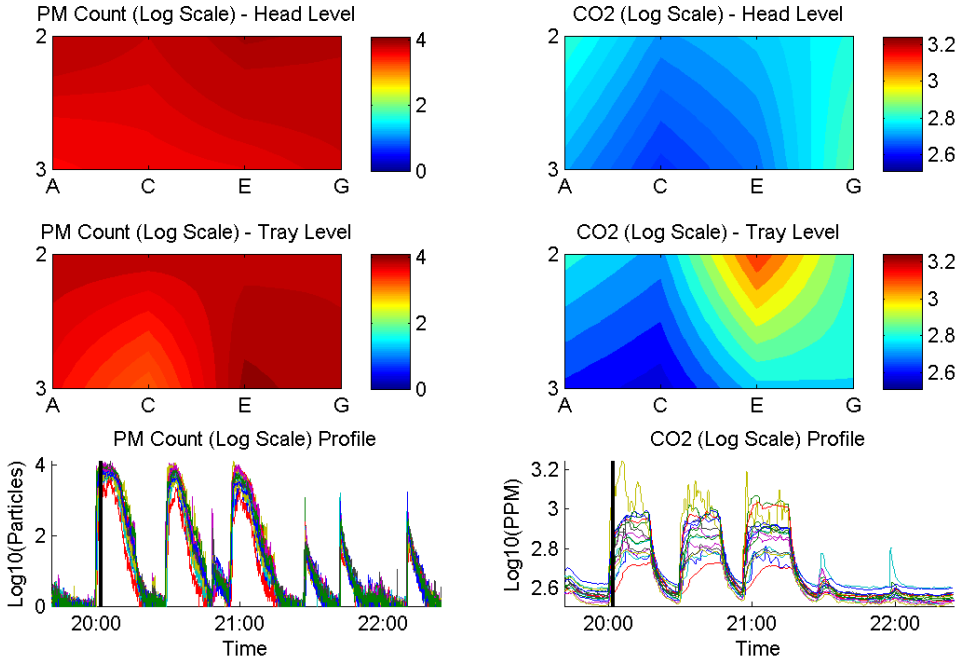

Figure 16: Three-dimensional smoke and CO_2 test with particulate and CO_2 contour plots at the height of contaminant injection.

more toward the sides of the cabin, with the contour lines running closer to parallel to the cabin centerline as opposed to what is seen with the particulate matter.

Figure 18 shows data from a point in time after the particulate matter concentration has peaked and is starting to be cleared out of the cabin by the ventilation system. The concentration of this contaminant appears to move away from the centerline, with the exception of a local maximum near the contaminant injection point. This peak may be due to residual smoke flushing from the injection system, or due to air being constrained by the seats in the cabin. The CO_2 again shows a trend at head-level to move toward the sides of the cabin away from the centerline. The largest peak remains at tray-level near the injection point, with a minimum that matches the particulate matter on the left side of the cabin at position 14. At this point in time there is a fairly good match in concentration distribution at the tray-level for both particulate matter and CO_2. This may suggest that, at this level, the airflow constraints caused by the cabin seating may be overcoming any differences between the sensor types within each node.

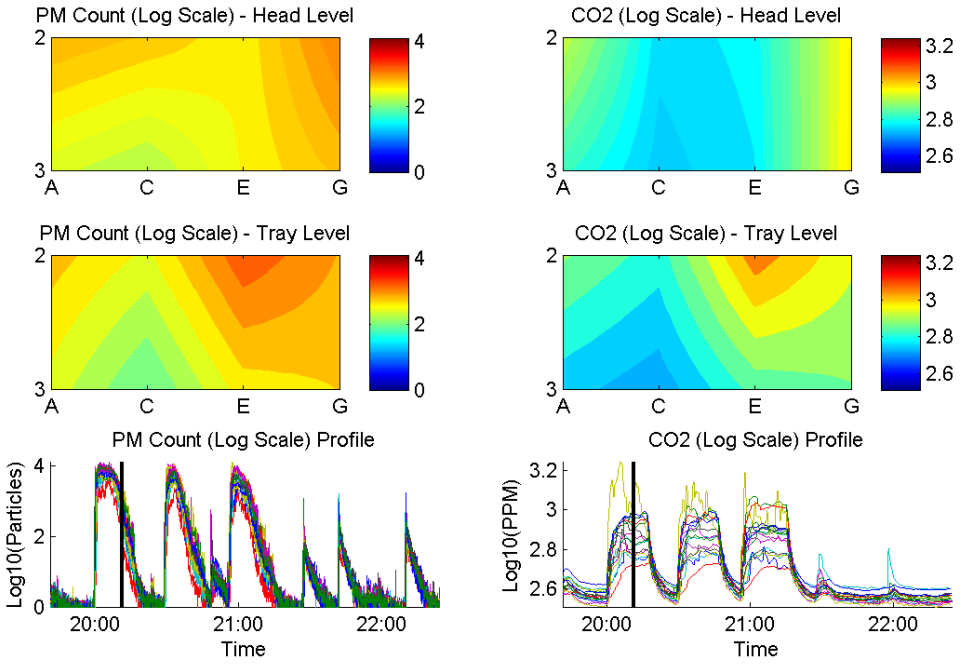

Figure 18: Three-dimensional smoke and CO_2 test with particulate and CO_2 contour plots as contaminant injection tapers off.

The KSU aircraft cabin simulator included the ability to test particulate matter using a talcum powder injection system that released particulate in a very short burst. The last two runs of the three-dimensional testing used this method for particulate matter injection without the use of CO_2. The injection points consisted of 7 nozzles across row 2 of the cabin, with one nozzle centered in each seat at a level just above the seat armrests.

Figure 20 shows the start of run 4, which is the first of the two talcum powder tests. The particulate matter first appears at the sensor nodes in row 2, which is where the talcum powder injection nozzles are located. It appears that, for both talcum powder runs, the sensors at positions 3 and 10 were the first to pick up the increase in particulate. The contaminant then moves over the seats to the sensors at head-level along row 3. This can be seen in Figure 21 where the concentrations are relatively high at head level along row 3 but remain lower at the tray-level. The minimum again appears at position 14 as it did when testing with smoke. Note that CO_2 never increases in the measurement area since it is not injected into the cabin during the talcum powder tests.

After the initial injection of particulate, the concentrations rapidly spread and begin to be removed by the ventilation system. Figure 22 shows the contour data as the concentrations abate. The particulate does appear to move outwards from the center to the sides as it is replaced by clean air from the ventilation system, again likely being pushed outward from the diffusers along the centerline.

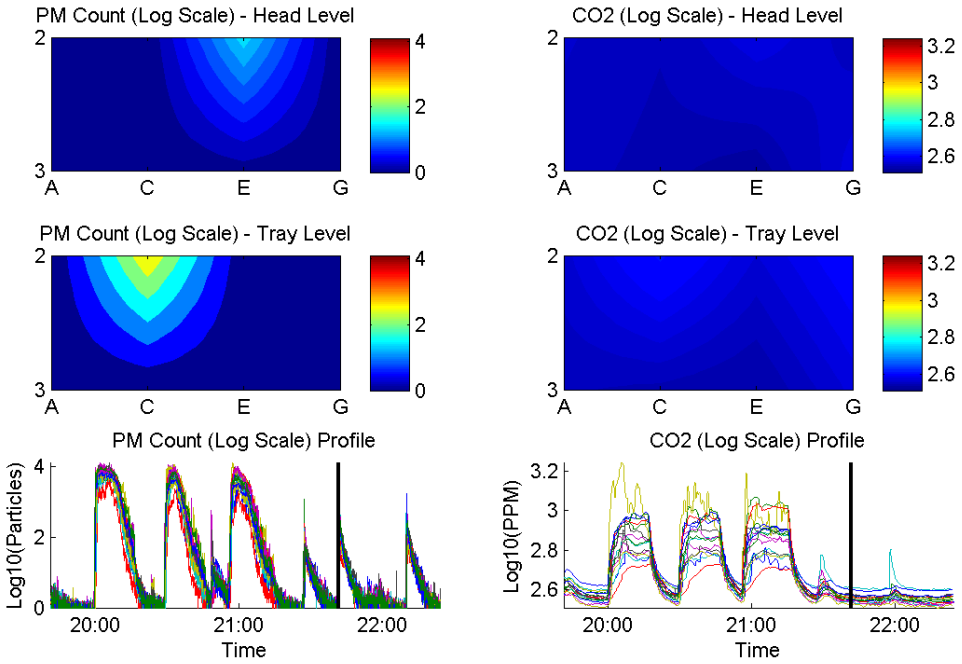

Figure 19: Three-dimensional talcum powder test with particulate and CO_2 contour plots at the start of contaminant injection.

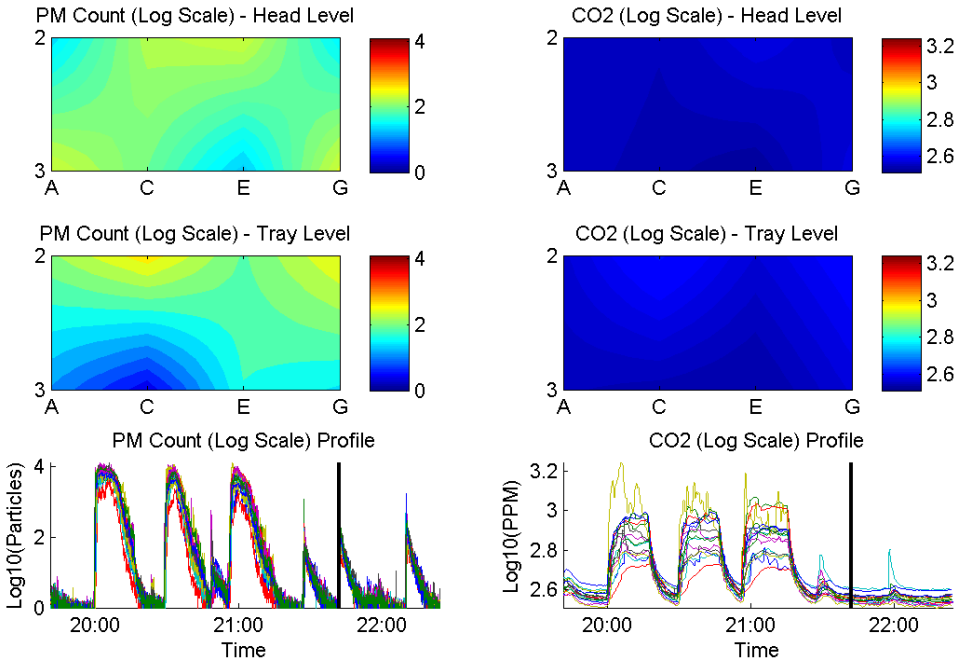

Figure 20: Three-dimensional talcum powder test with particulate and CO_2 contour plots as the contaminant spreads.

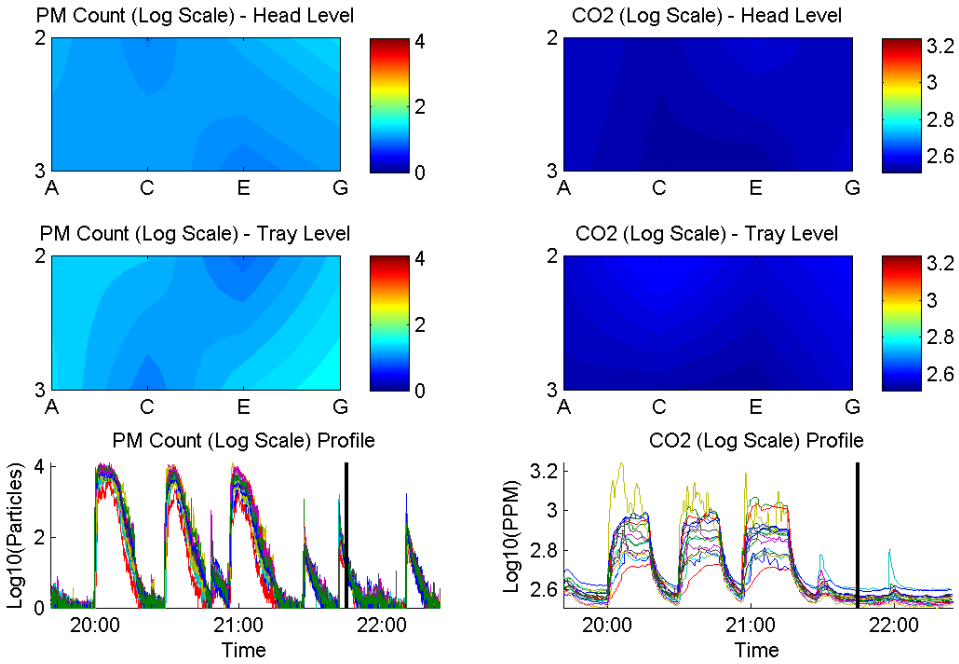

Figure 21: Three-dimensional talcum powder test with particulate and CO_2 contour plots near the end of contaminant injection.

It is not possible to make a qualitative comparison of the two different types of particulate matter contaminant used in the testing. The amounts and distributions of the two contaminants were quite different, and resulted in concentration peaks that were different by nearly two orders of magnitude. While there may be differences in the behavior of the two materials, further testing with similar concentrations and injection points would be required to make an attempt at any definitive statements along these lines.

VI. Conclusion

Advanced air quality measurement systems can bring visibility into complex environments where previously only single point measurements were available. These multi-point systems can track contaminants as they move through a space, allowing direct observation of their dispersal and providing significant data as to their sources. As demonstrated by the data above, the WAQM high-performance wireless data acquisition system may be used to meet the needs of aircraft bleed-air and environmental monitoring. This new system has been tested in a Boeing 767 mock-up cabin and has been shown to be capable of tracking multiple environmental variables simultaneously in two and three dimensions. The particulate matter sensor has shown itself capable of detecting different types of particulate matter from multiple sources. Spatial correlation has been demonstrated between two different airborne contaminants when released concurrently from the same location.

The flexibility of the WAQM wireless sensor network allows simple setup in configurations covering areas in two and three dimensions. Furthermore, the wireless sensor network can provide the necessary coverage and inter-node cooperation to effectively monitor the aircraft cabin environment. The inclusion of a particulate matter sensor coupled with contaminant localization will enable differentiation of bleed-air sourced and other cabin sourced contaminants. The WAQM system provides a new tool that will improve our ability to characterize and monitor air quality in the highly dynamic aircraft cabin environment.

VII. Acknowledgments

The authors would like to express their thanks to the staff of the Boise State University Hartman Systems Integration Laboratory for their contributions to the design and development of the Wireless Air Quality Monitor and its related systems. This work has been supported in part by the National Institutes of Health, National Children's Study, Mt. Sinai Contract # HHSN275201100002C / 0258-3624, and the Federal Aviation

Administration, Cooperative Agreement 10-C-RITE-BSU. Although the FAA has sponsored this project, it neither endorses nor rejects the findings of this research. The presentation of this information is in the interest of invoking technical community comment on the results and conclusions of the research.

The authors would like to thank Dr. Byron Jones and Michael Anderson of Kansas State University for the use of their facilities and equipment as well as their assistance with the experiments.

VIII. References

[1] National Research Council (US). Committee on Air Quality in Passenger Cabins of Commercial Aircraft, *The Airliner Cabin Environment and the Health of Passengers and Crew*, National Academies Press, 2002.

[2] Spengler, J. D., and Wilson, D. G., "Air quality in aircraft," *Proceedings of the Institution of Mechanical Engineers, Part E: Journal of Process Mechanical Engineering*, Vol. 217, No. 4, Jan. 2003, pp. 323–335.

[3] DeHart, R. L., "Health issues of air travel.," *Annual review of public health*, Vol. 24, Jan. 2003, pp. 133–51.

[4] Osman, S., La Duc, M. T., Dekas, A., Newcombe, D., and Venkateswaran, K., "Microbial Burden and Diversity of Commercial Airline Cabin Air During Short and Long Durations of Travel," *The ISME journal*, Vol. 2, No. 5, May 2008, pp. 482–497.

[5] Mcdevitt, J. J. et al., "Infectious Disease Transmission in Airliner Cabins." Report No. RITE-ACER-CoE-2012-01, 2012.

[6] Olsen, S. J. et al., "Transmission of the severe acute respiratory syndrome on aircraft.," *The New England journal of medicine*, Vol. 349, No. 25, Dec. 2003, pp. 2416–22.

[7] Pook, M., Loo, S. M., and Kiepert, J., "Monitoring of the Aircraft Cabin Environment via a Wireless Sensor Network," *AIAA 42nd International Conference on Environmental Sensing*, AIAA, 2012, pp. 1–9.

[8] Loo, S. M., Jones, B., Hall, J., Kiepert, J., and Anderson, M., "Bleed-Air Sensing: Particulate Matter Wireless Sensor Networks in Mock-up Cabin." Report No. RITE-ACER-CoE-2013-TBD, pp. 1–25, 2013.

[9] Hall, J. et al., "A Portable Wireless Particulate Sensor System for Continuous Real-Time Environmental Monitoring," *AIAA 42nd International Conference on Environmental Sensing*, AIAA, 2012, pp. 1–14.